Bull. Mater. Sci., Vol. 34, No. 4, July 2011, pp. 887–891. © Indian Academy of Sciences.

Synthesis and nonlinear optical characterization of new 1,3,4-oxadiazoles

B CHANDRAKANTHA, ARUN M ISLOOR[†,*], REJI PHILIP[††], M MOHESH[††], PRAKASH SHETTY[†††] and A M VIJESH

Syngene International Ltd, Biocon Park, Plot Nos 2 and 3, Bommasandra 4th Phase, Jigani Link Road, Bangalore 560 100, India

[†]Organic Chemistry Division, Department of Chemistry, National Institute of Technology Karnataka, Surathkal, Mangalore 575 025, India

[††]Light and Matter Physics Group, Raman Research Institute, C.V. Raman Avenue, Sadashiva Nagar, Bangalore 560 080, India

[†††]Department of Printing, Manipal Institute of Technology, Manipal University, Manipal 576 104, India

MS received 7 April 2010; revised 26 April 2010

Abstract. **A new series of 1,3,4-oxadiazole derivatives containing 2-fluoro-4-methoxy phenyl were synthesized by refluxing mixture of acid hydrazide 3 with different aromatic carboxylic acids (a–e) in phosphorous oxychloride. These newly synthesized compounds were characterized by NMR, mass spectral, and IR spectral studies, and also by C, H, N analyses. The open-aperture *z*-scan experiment was employed to measure the optical nonlinearity of the samples at 532 nm, using 5 ns laser pulses. The measurements indicate that compound 4a, which contains Bromine, behaves as an optical limiter at this wavelength, with potential applications in optoelectronics.**

Keywords. **1,3,4-Oxadiazole; nonlinear properties; *z*-scan; optical limiting.**

1. Introduction

Recently, organic molecules with significant nonlinear optical (NLO) properties have gained considerable importance due to their potential applications in optical data storage, optical communications, optical computing, optical switching, dynamic image processing, etc (Prasad and Williams 1991; Kanis *et al* 1994; Perry *et al* 1996; Sutherland 1996; Ronchi *et al* 2003). A large number of organic materials have therefore been investigated for their NLO properties. Due to their high molecular hyperpolarizabilities, organic materials display a number of interesting nonlinear optical effects. In addition to organics, a variety of inorganic and organometallic molecular systems also have been studied for NLO activity (Kanis *et al* 1994).

In general, the design strategy, used by many with success, involves connecting the donor (D) and acceptor (A) groups at the terminal positions of a *p*-bridge to create highly polarized molecules that can exhibit large molecular nonlinearity (Masraqui *et al* 2004). To date, the types of *p*-bridges investigated for developing efficient NLO materials and molecules include *D–A* olefines (Marder *et al* 1994; Blanchard-Desce *et al* 1995), acetylenes (Cheng *et al* 1991a), azo bridges (Moylan *et al* 1993), and aromatic (Cheng *et al* 1991b; Ruanwas *et al* 2010) and heteroaromatic rings (Rao *et al* 1993, 1994). Although push–pull polyenes generally show a large first hyperpolarizability, their thermal stability is not satisfactory. On the other hand, aromatic *D–A* molecules are more stable but they exhibit relatively lower hyperpolarizability values. Another observed issue is that the incorporation of benzene rings into the aliphatic push–pull polyenes results in saturation of the molecular nonlinearity (Varanasi *et al* 1996). To overcome this problem, several groups (Rao *et al* 1993, 1994; Varanasi *et al* 1996) have developed NLO chromophores containing easily polarizable five membered heteroaromatic rings. Heterorings such as furan and thiophene, due to their relatively lower aromatic stabilization energy than benzene, are reported to provide more effective *p*-conjugation between *D* and *A*, resulting in larger nonlinearities (Varanasi *et al* 1996).

In search of new NLO materials among heterocyclic compounds, here we have used the 1,3,4-oxadiazole ring as a *p*-bridge on the grounds that its reduced aromaticity may offer better prospects for *p*-electron delocalization across the *D–A* links. Substitutions at the 2 and 5 positions of the oxadiazole core were made to ensure that the oxadiazole core, indeed, acts as a *p*-conjugated backbone. The third order optical nonlinearity in these molecules were investigated by the open aperture *z*-scan experiment. Various aromatic donors and acceptors

*Author for correspondence (isloor@yahoo.com)

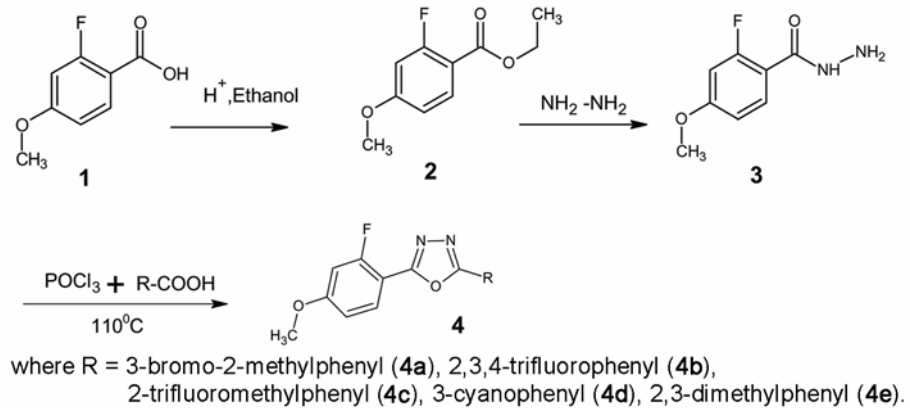

Figure 1. Scheme for synthesis of oxadiazole derivatives.

were used to tune the electronic factor and understand the origin of the nonlinearity in these molecules.

2. Experimental

Infrared spectra of all intermediate and final compounds were recorded on a Nicolet Avatar 5700 FTIR (Thermo Electron Corporation) spectrometer. The UV-Vis and fluorescence emission spectra of the 1,3,4-oxadiazoles were measured in GBC Cintra 101 UV-Vis and PerkinElmer LS55 spectrophotometers respectively. ^{1}H NMR spectra were obtained with AMX 400 MHz FT-NMR spectrophotometer using TMS/solvent signal as internal reference. Mass spectra were recorded on a Jeol SX-102 (FAB) Mass Spectrometer. Elemental analysis was performed on a Flash EA1112 C, H, N, S analyzer (Thermo Electron Corporation).

2.1 *Synthesis of 1,3,4-oxadiazoles*

2.1a *Preparation of ethyl 2-fluoro-4-methoxybenzoate* (**2**): To a mixture of 2-fluoro-4-methoxybenzoic acid (**1**, 10 g, 0·0587 mol) in ethanol (100 ml) conc. sulphuric acid (1 ml) was added and refluxed for 5 h. The reaction mixture was concentrated, the solid separated was filtered, washed with water, and recrystalised with ethanol to give **2** as white crystals (10 g, 85%) m.p. 200–223°C.

2.1b *Preparation of 2-fluoro-4-methoxybenzohydrazide* (**3**): A mixture of ethyl 2-fluoro-4-methoxybenzoate (**2**, 10 g, 0·0504 mol) and hydrazine hydrate (5·0 ml, 0·1009 mol) in ethanol (100 ml) was heated under reflux for 8 h. The reaction mixture was concentrated and left to cool. The solid product obtained was filtered, washed with water and recrystallised with ethanol to give **3** as white crystals. (7 g, 89%), m.p. 240–243°C.

2.1c *General procedure for preparation of 2-(2-fluoro-4-methoxyphenyl)-5-substituted 1, 3,4-oxadiazole* (**4**): A mixture of acid hydrazide **3** with different aromatic carboxylic acids (a–e) was refluxed with phosphorous oxychloride (10 vol) for 3 h. Reaction mixture was concentrated using rotor evaporator, the residue was quenched with ice water and the solid separated was filtered off, washed with water and further purified by recrystallization with ethanol to afford 5-substituted 1,3,4-oxadiazole bearing 2-fluoro-4-methoxy phenyl moiety as white crystalline solid.

2.2 *Characterization data for the newly synthesized molecules (***4a**–**4e***)*

Compound **4a**: (1·5 g, 78%); m.p. 290–295°C; IR (KBr) cm^{-1} 3097 (Ar-H), C=N (1594), C=C (1560), C–O (1057, stretch of oxadiazole ring), C–F (1093); mass *m*/*z* (M^+) 364: ^{1}H NMR (300 MHz-DMSO d_6-ppm) δ 8·02–8·07 (*m*, 1H, Ar-H), 7·95–7·98 (*d*, 1H, Ar-H, *J* = 7·8 Hz), 7·87–7·89 (*d*, 1H, Ar-H, *J* = 7·14 Hz), 7·34–7·39 (*m*, 1H, Ar-H), 7·10–7·16 (*dd*, 1H, Ar-H, *J* = 2·4 Hz), 7·00–7·04 (*dd*, 1H, Ar-H, *J* = 2·31 Hz), 3·87 (*s*, 3H, –OCH_3), 2·73 (*s*, 3H, –CH_3) Anal. found (calc.) for $C_{16}H_{12}BrFN_2O_2$ (%): C, 53·01 (52·91); H, 3·45 (3·29); N, 7·96 (7·8).

Compound **4b**: (1·6 g, 90%); m.p. 235–238°C; IR (KBr) cm^{-1} 3070 (Ar-H), C=N (1585), C=C (1580), C–O (1040, stretch of oxadiazole ring), C–F (1090); mass *m*/*z* (M^+) 325: ^{1}H NMR (300 MHz–DMSO-d_6-ppm) δ 8·04–8·09 (*t*, 1H, Ar-H, *J* = 8·5 Hz), 7·91–7·93 (*m*, 1H, Ar-H), 7·15–7·19 (*m*, 1H, Ar-H), 6·77–6·89 (*m*, 2H, Ar-H), 3·9 (*s*, 3H, –OCH_3). Anal. found (calc.) for $C_{15}H_8F_4N_2O_2$ (%): C, 55·65 (55·56); H, 2·60 (2·47); N, 8·78 (8·64).

Compound **4c**: (1·5 g, 81%); m.p. 222–228°C; IR (KBr) cm^{-1} 3070 (Ar-H), C=N (1545), C=C (1560), C–O (1070, stretch of oxadiazole ring), C–F (1050); mass *m*/*z* (M^+) 339: ^{1}H NMR (400 MHz–DMSO-d_6-ppm). δ 8·34–8·39 (*m*, 2H, Ar-H), 8·07–8·11 (*m*, 1H, Ar-H), 7·81–7·83 (*m*, 1H, Ar-H), 7·67–7·71 (*m*, 1H, Ar-H), 6·79–6·89 (*dd*, 2H,

Ar-H, J = 8·8 Hz), 3·9 (*s*, 3H, –OCH_3). Anal. found (calc.) for $C_{16}H_{10}F_4N_2O_2$ (%): C, 57·01 (56·91); H, 2·18 (3·00); N, 8·43 (8·3).

Compound **4d**: (1·5 g, 81%); m.p. 222–228°C; IR (KBr) cm^{-1} 3030 (Ar C–H), C=N (1615), C=C (1540), C–O (1060, stretch of oxadiazole ring), C–F (1070); mass *m*/*z* (M^+) 296: ^{1}H NMR (400 MHz-DMSO-d_6-ppm). δ 8·39–8·41(*m*, 2H, Ar-H), 8·11–8·17 (*m*, 2H, Ar-H), 7·82–7·86 (*m*, 1H, Ar-H), 7·14–7·18 (*dd*, 1H, Ar-H, J = 2·4 Hz), 7·03–7·06 (*dd*, 1H, Ar-H, J = 2·4 Hz), 3·89 (*s*, 3H, –OCH_3). Anal. found (calc.) for $C_{16}H_{10}FN_3O_2$ (%): C, 65·29 (65·09); H, 3·51 (3·39); N, 14·23 (14·44).

Compound **4e**: (1·5 g, 92%); m.p. 222–228°C; IR (KBr) cm^{-1} 3020 (Ar C–H), C=N (1615), C=C (1540), C–O (1060, stretch of oxadiazole ring), C–F (1070); mass *m*/*z* (M^+) 299: ^{1}H NMR (300 MHz–DMSO d_6-ppm). δ 8·04–8·10 (*t*, 1H, Ar-H, J = 8·52 Hz), 7·80–7·82 (*d*, 1H, Ar-H, J = 7·59 Hz), 7·24–7·35 (*m*, 2H, Ar-H) 6·76–6·88 (*m*, 2H, Ar-H), 3·89 (*s*, 3H, –OCH_3), 2·65 (*s*, 3H, –CH_3), 2·40 (*s*, 3H, –CH_3) Anal. found (calc.) for $C_{17}H_{15}FN_2O_2$ (%): C, 68·65 (68·55); H, 5·38 (5·09); N, 9·64 (9·50).

3. Results and discussion

The formation of oxadiazole **4a** was confirmed by recording its IR, NMR and mass spectra. IR spectrum of oxadiazole showed the Ar–H band at 3097 cm^{-1}, C=N band at 1594 cm^{-1}, C=C band at 1560 cm^{-1} and C–F band at 1093 cm^{-1}. The stretch of oxadiazole ring appeared at 1057 cm^{-1} due to C–O. Mass spectrum of **4a** showed molecular ion peak m/z (M^+) 364. ^{1}H-NMR spectrum showed multiplet in the region of δ, 7–8·07. A singlet appearing at δ, 3·87 is due to three protons of –OCH_3. Scheme for synthesis of the oxadiazole derivatives is given in figure 1, physical data and spectral details of remaining compounds are presented.

For the *z*-scan, samples dissolved in chloroform were taken in 1 mm path length cuvettes, and irradiated by laser pulses of 90 microjoules energy and 5 nanoseconds duration at the wavelength of 532 nm. The laser pulses were obtained from the second harmonic output of an Nd : YAG laser (Continuum, MiniLite). Of all the samples investigated, sample **4a**, which contains Bromine, showed maximum optical nonlinearity. As seen from the open aperture *z*-scan curve given in figure 2, the optical transmission of sample **4a** is reduced at higher laser intensities, showing that the sample behaves as an optical limiter. The UV-Vis spectrum of sample **4a** depicted in figure 3 shows a single absorption band that peaks near 350 nm, and the absorption is very weak at the excitation wavelength of 532 nm. Indeed our sample had a high linear transmission of 83% at the excitation wavelength. This reduced to 54% at maximum laser intensity used i.e. when the sample was at the beam focus in the *z*-scan. It is well known that optical limiters are potentially useful in protecting human eyes and other light sensitive devices like cameras from accidental exposure to intense light.

Since the sample had a high transmission at the excitation wavelength, from a first approximation it could be surmised that the cause of the observed optical limiting is two-photon absorption (TPA). Therefore we tried to fit the *z*-scan data to the standard nonlinear transmission equation for a TPA process, given by Sheik Bahae *et al* (1990). Even though a good fit was obtained, it became clear that absorption saturation in the sample also should be considered to obtain the best fit. Hence an effective nonlinear absorption coefficient $\alpha(I)$, given by

$$\alpha(I) = \frac{\alpha_0}{1+(I/I_s)} + \beta I, \tag{1}$$

has been considered, where α_0 is the unsaturated linear absorption coefficient at the wavelength of excitation, and I_s is the saturation intensity (intensity at which the linear absorption drops to half its original value) and βI is the TPA coefficient. For calculating the transmitted intensity for a given input intensity, we numerically solve the propagation equation

$$\frac{dI}{dz'} = -\left[\left(\alpha_0 \Big/ \left(1+\frac{I}{I_s}\right)\right) + \beta I\right] I, \tag{2}$$

using the fourth order Runge–Kutta method. Here z' indicates the propagation distance within the sample. Input intensities for the gaussian beam for each sample position in the *z*-scan are calculated from the input energy, laser pulse width and irradiation area. Finally, the normalized

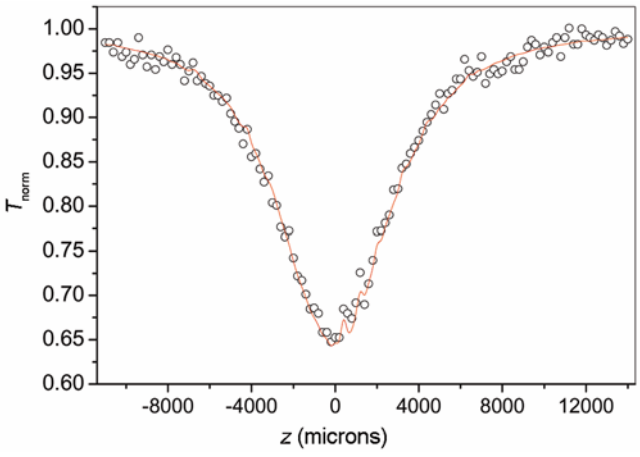

Figure 2. The open aperture z-scan curve of sample **4a**. At the maximum laser intensity used (z = 0), the normalized transmittance of the sample has reduced to 0·65. Circles are data points while the solid curve is a numerical fit using (2).

transmittance is calculated by dividing the output intensity with the input intensity and normalizing it with the linear transmittance. As seen from figure 2, there is excellent agreement between the experimental data and numerical simulation. The numerically estimated values of β and I_s are $3{\cdot}3 \times 10^{-11}$ m/W and 8×10^{12} W/m^2 respectively.

It may be noted that in molecular systems the possibility of excited state absorption (ESA) is much stronger when excited with nanosecond laser pulses, compared to shorter (picoseconds and less) laser pulses. Even though the excited state population will be low in the present case due to the weak absorption at 532 nm, ESA cross-sections are much larger than genuine TPA cross-sections in general, and hence cannot be ignored. Therefore β will have contributions from genuine TPA as well as ESA effects. Under similar excitation conditions, NLO materials like Cu nanocomposite glasses gave β values of 10^{-10}–10^{-12} m/W (Karthikeyan *et al* 2008), bismuth nanorods gave $5{\cdot}3 \times 10^{-11}$ m/W (Sivaramakrishnan *et al* 2007) and CdS quantum dots gave $1{\cdot}9 \times 10^{-9}$ m/W (Kurian *et al* 2007) respectively. These values show that the present samples have an optical nonlinearity comparable to these recently investigated nanomaterials. Figures 4–7 are the *z*-scan measurements for the compounds **4** (b–e), which indicate that **4a** is an interesting molecule.

4. *z*-Scan measurement

We employed the open-aperture *z*-scan experiment (Varanasi *et al* 1996) to measure the optical nonlinearity of the newly synthesized compounds. In the open aperture *z*-scan, which gives information about the nonlinear absorption coefficient, a focused laser beam is passed through the sample under study. The direction of propagation of the beam is taken as the *z*-axis. The beam will

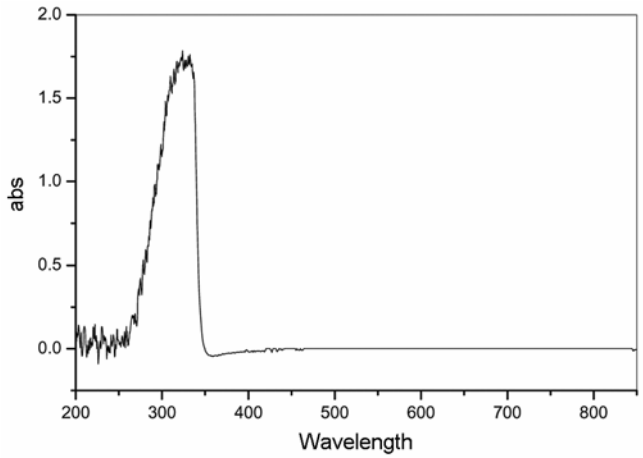

Figure 3. UV-Vis spectrum of sample **4a**.

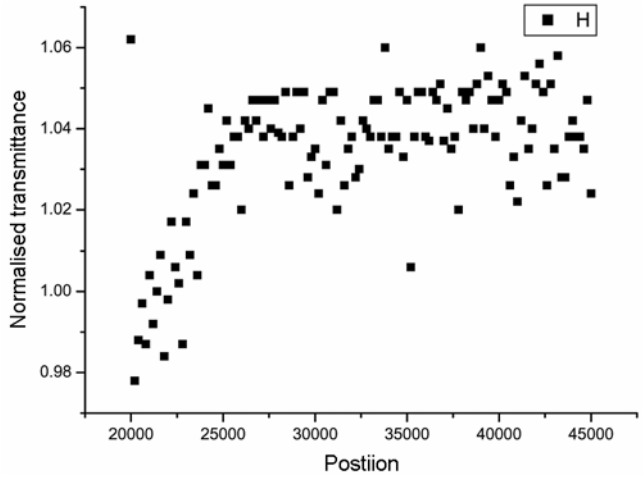

Figure 4. The open aperture z-scan curve of sample **4b**.

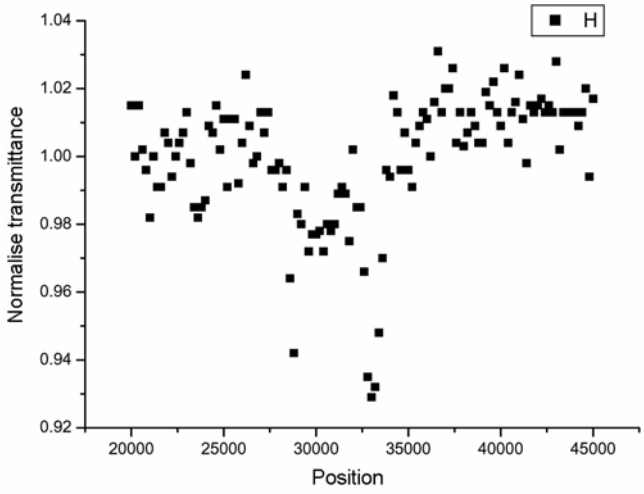

Figure 5. The open aperture z-scan curve of sample **4c**.

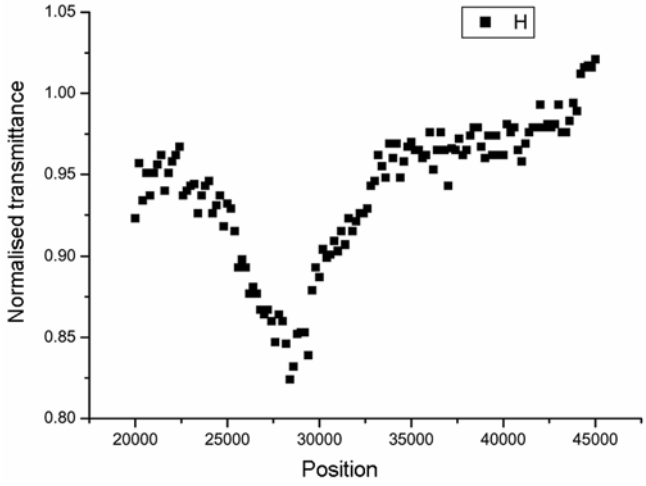

Figure 6. The open aperture z-scan curve of sample **4d**.

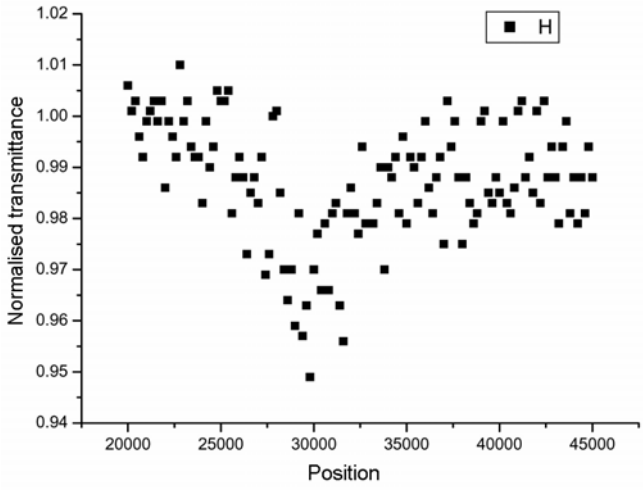

Figure 7. The open aperture z-scan curve of sample **4e**.

have maximum energy density at the focus, which is taken as $z = 0$. The energy density will symmetrically reduce towards either side of the focal point (i.e. for the positive and negative values of z). The experiment is done by placing the sample in the beam at different positions with respect to the focus, and measuring the corresponding light transmission. The nonlinear absorption coefficient can be calculated by fitting the z-scan curve to standard nonlinear transmission equations.

5. Conclusions

We have synthesized new oxadiazole derivatives which were characterized by IR, NMR and mass spectral studies. The optical nonlinearity of the compounds was measured at 532 nm using 5 ns laser pulses, employing the open aperture z-scan technique. Sample **4a** which contains bromine has shown a substantial optical limiting property, comparable in magnitude to previously investigated metal nanocomposites and nanorods. This material may have potential applications in optical limiting devices.

Acknowledgements

A M I is thankful to the HOD Chemistry and Prof Sandeep Sancheti, Director, National Institute of Technology–Karnataka, Surathkal India for providing research facilities and encouragement. R P thanks C S Suchand Sandeep for help with z-scan measurements.

References

Blanchard-Desce M, Runser C, Fort A, Barzoukas M, Lehn J -M, Ploy V and Alain V 1995 *Chem. Phys.* **199** 253

Cheng L -T, Tam W, Marder S R, Stiegman A E, Rikken G and Spangler C W 1991b *J. Phys. Chem.* **95** 10643

Cheng L -T, Tam W, Stevenson S H, Meredith G R, Rikken G and Marder S R 1991a *J. Phys. Chem.* **95** 10631

Kanis D R, Ratner M A and Marks T J 1994 *Chem. Rev.* **94** 195

Karthikeyan B, Anija M, Sandeep C S, Nadeer T M and Philip R 2008 *Optics Commun.* **281** 2933

Kurian P A, Vijayan C, Sathiyamoorthy K, Sandeep C S and Philip R 2007 *Nanoscale Res. Letts.* **2** 561

Marder S R, Cheng L -T, Tiemann B G, Friedli A C, Blanchard-Desce M, Perry J W and Skindho J 1994 *Science* **263** 511

Masraqui S H, Kenny R S, Ghadigaonkar S G, Krishnan A M Bhattacharya and Das P K 2004 *Opt. Mater.* **27** 257

Moylan C R, Twieg R J, Lee V Y, Swanson S A, Betterton K M and Miller R D 1993 *J. Am. Chem. Soc.* **115** 12599

Perry J W, Mansour K, Lee I -Y S, Wu X -L, Bedworth P V, Chen, C -T, Ng D, Marder S R, Miles P, Wada T, Tian M and Sasabe H 1996 *Science* **273** 1533

Prasad P N and Williams D J 1991 *Introduction to nonlinear optical effects in molecules and polymers* (New York: Wiley)

Rao V P, Cai Y M and Jen A K Y 1994 *Chem. Comm.* 1689

Rao V P, Jen A K Y, Wong K Y and Drost K J 1993 *Chem. Comm.* 1118

Ronchi A, Cassano T, Tommasi R, Babudri F, Cardone A, Farinola G M and Naso F 2003 *Synth. Met.* **139** 831

Ruanwas P, Kobkeatthawin T, Chantrapromma S, Fun H K, Philip R, Smijesh N, Padaki M and Isloor A M 2010 *Synth. Met.* **160** 819

Sheik Bahae M, Said A A, Wei T M, Hagan D J and Van Stryland E W 1990 *IEEE J. Quant. Electron.* **26** 760

Sivaramakrishnan S, Muthukumar V S, Sivasankara Sai S, Venkataramanaiah K, Reppert J, Rao A M, Anija M, Philip R and Kuthirummal N 2007 *Appl. Phys. Letts.* **91** 093104

Sutherland R L 1996 *Handbook of nonlinear optics* (New York: Dekker

Varanasi P R, Jen A K Y Chandrasekhar J, Namboothiri I N N and Rathna A 1996 *J. Am. Chem. Soc.* **118** 12443